Available online at www.sciencedirect.com
ScienceDirect
Earth and Planetary Science Letters 252 (2006) 162–179
EPSL
www.elsevier.com/locate/epsl

A stacked record of relative geomagnetic paleointensity for the past 270 kyr from the western continental rise of the Antarctic Peninsula

Patrizia Macrì [a,*], Leonardo Sagnotti [a], Renata Giulia Lucchi [b], Michele Rebesco [c]

[a] Istituto Nazionale di Geofisica e Vulcanologia, Via di Vigna Murata 605, 00143 Roma, Italy
[b] GRC Geociències Marines, Departament d'Estratigrafia, P. i Geociències Marines, Universitat de Barcelona, C/ Martí i Franquès, s/n, E-08028, Barcelona, Spain
[c] Istituto Nazionale di Oceanografia e di Geofisica Sperimentale (OGS), Borgo Grotta Gigante 42/c, 34010 Sgonico (Trieste), Italy

Received 12 April 2006; received in revised form 20 September 2006; accepted 20 September 2006
Available online 7 November 2006
Editor: M.L. Delaney

Abstract

Paleomagnetic and rock magnetic investigations were carried out on four gravity cores recovered from the western continental rise of the Antarctic Peninsula during the SEDANO II cruise of RV OGS-Explora. The studied cores, each about 6.5 m-long, were collected at a depth of 3700–4100 m below the sea level, on the distal gentle side of sediment Drift 7, and consist of very fine-grained sediments spanning through various glacial–interglacial cycles. Detailed analysis of the paleomagnetic and rock magnetic data allowed to reconstruct relative paleointensity (RPI) records ($NRM_{20\ mT}/ARM_{20\ mT}$) for each core. We established a refined age model for the studied sequences by correlating individual SEDANO RPI curves to the global RPI stack SINT-800 [Y. Guyodo, J.-P. Valet, Global changes in intensity of the Earth's magnetic field during the past 800 kyr, Nature 399 (1999) 249–252]. The individual normalized SEDANO RPI records are in mutual close agreement; they were thus merged in a RPI stacking curve spanning the last 270 kyr and showing a low standard deviation. This study also points out that RPI records may provide a viable tool to date otherwise difficult-to-date sedimentary sequences, such as those deposited along peri-Antarctic margins. The new RPI chronology indicates that the sampled sedimentary sequence is younger than previously thought and allows a new high-resolution correlation to oxygen isotope stages. Furthermore, we recognized variations in the rock magnetic parameters that appear to be climatically-driven, with changes in the relative proportion of two magnetic mineral populations with distinct coercivities. Rock magnetic and lithological trends observed in the SEDANO cores indicate that during the climatic cycles of the Late Pleistocene this sector of the peri-Antarctic margin was subjected to subtle, yet identifiable, environmental changes, confirming a relatively higher instability of the West Antarctic ice sheet with respect to the East Antarctic counterpart.

Keywords: Paleomagnetism; Geomagnetic relative paleointensity; Environmental magnetism; Antarctica

1. Introduction

Since the late 1970's geomagnetic relative paleointensity (RPI) records, obtained from worldwide distributed Late Pleistocene marine sedimentary sequences [i.e., 1–13], demonstrated their potentiality as a

* Corresponding author. Tel.: +39 0651860700; fax: +39 0651860397.
E-mail address: macri@ingv.it (P. Macrì).

0012-821X/$ - see front matter © 2006 Elsevier B.V. All rights reserved.
doi:10.1016/j.epsl.2006.09.037

powerful high-resolution tool for stratigraphic correlations of sedimentary sequences deposited during the Brunhes Chron.

Following the development of the research, synthetic global RPI stack curves were progressively compiled for the last 200 kyr (SINT-200 [14]) and 800 kyr (SINT-800 [15]) and successively refined for the last 75 kyr with RPI stacks both at regional and global scales (NAPIS-75 [16], SAPIS [17] and GLOPIS-75 [18]). These synthetic RPI stacks provide target curves for correlating individual RPI records and to tie them to the SPECMAP orbitally tuned $\delta^{18}O$ reference curve [19–21].

Other RPI records and stack curves expand detailed RPI reconstructions to older time intervals back in to the Matuyama Chron [22–30].

Generally RPI curves from different regions show a mutual good agreement on the main long period features, but they often disagree on the amplitude of the individual highs and lows and on high-frequency features. Discrepancies may be caused by uncorrected environmental factors, local geomagnetic field effects, differences in the paleomagnetic lock-in depth functions [31,32], or by some shift in ages between cores due to an incomplete knowledge of the age to depth relationship in the sedimentary sequences [33].

The available RPI records, though effectively spread on a worldwide distribution, refer mostly to low- and mid-latitudes. Only a few RPI curves were recently obtained from high-latitudes of the Southern Hemisphere [11,17,27,34–38]. Anyway, a proper reconstruction of the relative geomagnetic dipole strength variation during geological past needs plenty of experimental evidences, also from the polar regions. For this reason, the construction of RPI records from marine sediments of the peri-Antarctic margins must be regarded as a good chance for the establishment of an ever more accurate reconstruction of past geomagnetic dipole intensity variations.

Furthermore, RPI records can be used as a stratigraphic tool to solve chronological uncertainties in deep sea sedimentary record of the Southern Ocean south of the polar front. These records have been often neglected from paleoceanographic studies because Antarctic deep and bottom waters are corrosive with respects to biogenic carbonate, and the resulting stratigraphy is deprived of the paleoenvironmental and age proxies derived from the stable isotopes composition of oxygen and carbon in foraminiferal skeletons. In this context, RPI studies may provide a unique and original age model, at high-resolution, to which refer the occurrence of geological and climatic events as recorded in the sedimentary sequences deposited in the peri-Antarctic margins.

In this work, we present the RPI data of four SEDANO II cores, collected from the continental rise of the Pacific margin of the Antarctic Peninsula (Fig. 1). The aim was to extend back in time the RPI records that were previously obtained in the same area, spanning a sedimentary record limited to the last glacial–interglacial cycle (i.e. the last 80 kyr) in two cores and extended to the past 160 kyr in only one core [34].

The new RPI records expand the reconstruction of the relative variation of the geomagnetic field intensity to the last three full glacial–interglacial cycles and can be merged to compile a synthetic stacked RPI record for this sector of the peri-Antarctic margin, spanning the last 270 kyr.

The reconstructed RPI curves are then used to address chronostratigraphic problems in the sampled sequence and to establish an original high-resolution age model for the cores. Finally, we will discuss the effects of climatic changes on the magnetic mineralogy of the sedimentary sequence.

2. Geological setting and lithostratigraphy

The depositional system of continental rise in the Pacific continental margin of the Antarctic Peninsula is formed by a system of nine sedimentary Drifts having main-elongated axis perpendicular to the margin, and separated from the continental slope by a trough representing a zone of erosion (Fig. 1). Between Drifts are large channel systems originated by turbidity currents [39,40].

Multi-channel seismic reflection profiles acquired over the continental rise, show that the larger hemipelagic sediment Drifts (approximately 100 km long, 50 km wide and with more than 1 km of elevation), have a characteristic asymmetric cross section, with a steep SW side and a gently sloping NE side as results of a south-westward transport and deposition operated by bottom contour currents, that rework fine sediments delivered into the system mainly by turbidity currents and meltwater turbid plumes [39–42].

Five depositional settings have been distinguished within Drift 7 [40,41], including: (1) Alexander deep sea channel system, where the sedimentation is directly influenced by turbidity currents; (2) NE gentle slope of the Drift facing the Alexander channel system, where the sedimentation is mainly due to turbid meltwater plumes and ice-rafted/wind-transported detritus; (3) proximal crest of the Drift, where the sedimentation is mainly due to turbid plumes and ice-rafted/wind-transported detritus; (4) distal part of the Drift, with sedimentation dominated by contour currents and occasionally by distal

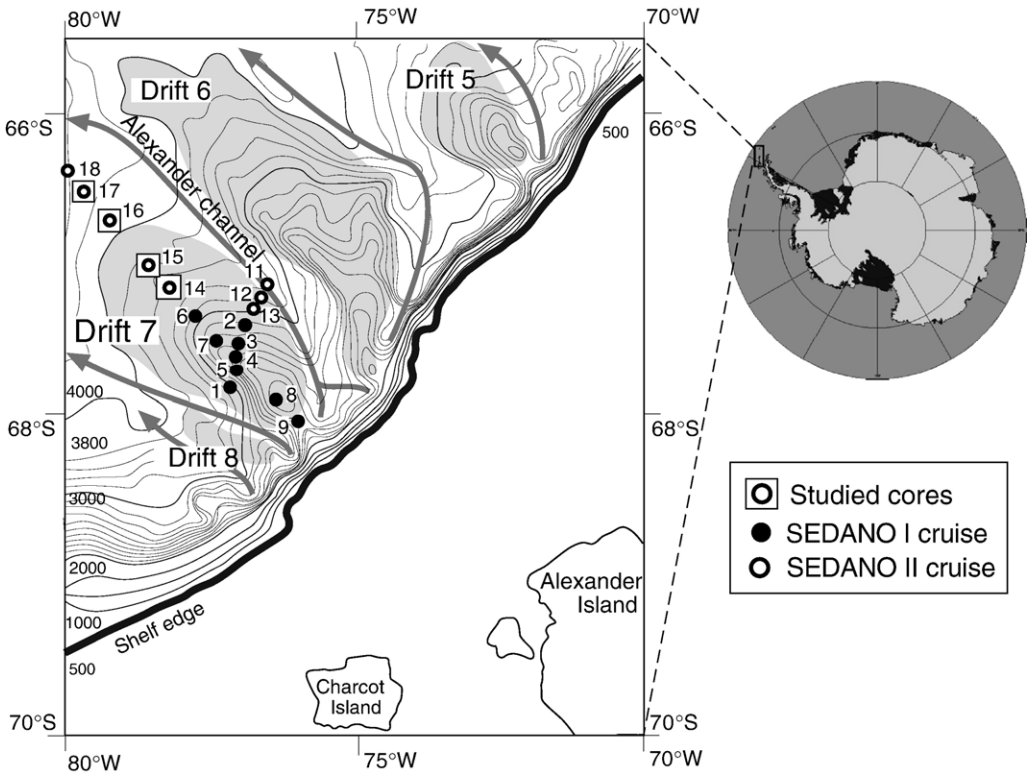

Fig. 1. Location of the studied SEDANO cores (SED-14, SED-15, SED-16 and SED-17) collected on the continental rise of the Pacific margin of the Antarctic Peninsula. The studied cores are aligned along the elongation axis of the sediment Drift 7, on the distal side sloping toward the abyssal plain. The study area is centered at about 67°20′ Lat S and 77°20′ Lon W, and the cores were recovered at depths of 3700–4100 m below the sea level.

turbidity flows; (5) steep SW side of the Drift, where the sedimentation is disturbed by local mass instability and reworking by contour currents that deplete the deposits from the fine fraction.

The four deep-sea gravity cores investigated in this study were collected, within the SEDANO (SEdiment Drifts of the ANtarctic Offshore) project, on the long axis of the Drift 7, in the distal area towards the abyssal plain, and consist of mud sequence with few silty layers. Their position (Fig. 1) is the following: core SED-14 (67°06.82′ S–78°10.48′ W, 3768 m water depth), SED-15 (66°58.96′ S–78°29.30′ W, 3880 m water depth), SED-16 (66°41.85′ S–79°09.60′ W, 4055 m water depth) and SED-17 (66°32.94′ S–79°29.03′ W, 4130 m water depth).

The stratigraphic framework of the SEDANO cores was formerly studied and described in detail [41–44]. The Pleistocene sequence of Drift 7 was subdivided in nine lithostratigraphic units, named from A to I, and tentatively correlated to Oxygen Isotope Stages (OIS) from 1 to 11 (see Fig. 2 in Lucchi et al. [41]). On the basis of micropalaeontological, compositional and sedimentological evidences, a link between paleoclimate and lithostratigraphy has been originally developed for units from A to C [41,43,44]. Interglacial intervals were recognized as consisting of brown bioturbated, diatom-bearing hemipelagic sediments with sparse ice rafted debris, foraminifera and radiolarians, while intervals of grey laminated, barren sediments with millimeter-thick silty laminae were referred to glacial periods [43]. The interglacial unit C was correlated to OIS 5 on the basis of micropaleontological content that include planktonic foraminifera and calcareous nannofossils. The presence of the latter is restricted to this interval, suggesting dating of the unit C boundaries at ca. 127 and 70 ka [45].

The stratigraphy older than unit C appears more uncertain and has been developed on the basis of lithological and textural characteristics, magnetic susceptibility logs, compositional and biostratigraphic content of the sediments, though the biostratigraphic record is discontinuous [45].

A 3 cm thick tephra layer, recognized at the bottom of the interglacial unit C, represents a fine point of correlation among the various SEDANO cores [41–43]. Thirteen discrete volcanic ash layers (tephra) were identified in the last 200 kyr section of the EPICA-Dome

C ice record [46,47]. Two of these tephra layers, with volcanic sources identified in the inland volcanic provinces of Marie Byrd Land and McMurdo and dated at ca. 129.5 ka and 139.6 ka [47,48], were also recognized in the offshore sediments of the northern Antarctic Peninsula [41–43].

Previous high-resolution RPI dating of SED-02, SED-04 and SED-06 cores, spanning through units A–C and reaching unit D in core SED-06 only [34], pointed out the occurrence within unit B (corresponding to OIS from 2 to 4) of characteristic decimeter-thick dark grey mud layers which appear almost coeval to the millennial-scale Heinrich events, recognized in the North Atlantic sediments as episodes of increased iceberg discharge [49–51], and appear therefore as local climatic proxies [34].

3. Sampling, methods and measurements

In February 2005, 1-m long u-channel samples were collected from the archives halves of the SED-14, SED-15, SED-16 and SED-17 core sections, at the Core Repository of the "Sorting Centre" of the Italian *Museo Nazionale dell'Antartide* in Trieste. Magnetic data were acquired at the paleomagnetic laboratory of the *Istituto Nazionale di Geofisica e Vulcanologia* in Rome, where the u-channels were measured in a magnetically shielded room using an automated pass through 2-G Enterprises DC SQUID cryogenic magnetometer system, with in-line a Bartington MS2C susceptibility loop sensor, a set of three orthogonal alternating field (AF) demagnetizing coils with optional anhysteretic remanent magnetization (ARM) capabilities, and an isothermal remanent magnetization (IRM) pulse magnetizer.

The u-channels were measured at 1-cm spacing in order to obtain high-resolution records of the natural remanent magnetization (NRM), ARM and the low-field volume specific magnetic susceptibility (κ). However, the half-width of the response function of the pick-up coils in the DC SQUID cryogenic magnetometer is of 4.5 cm, so that remanence values on the u-channel samples are truly independent every ca. 5 cm.

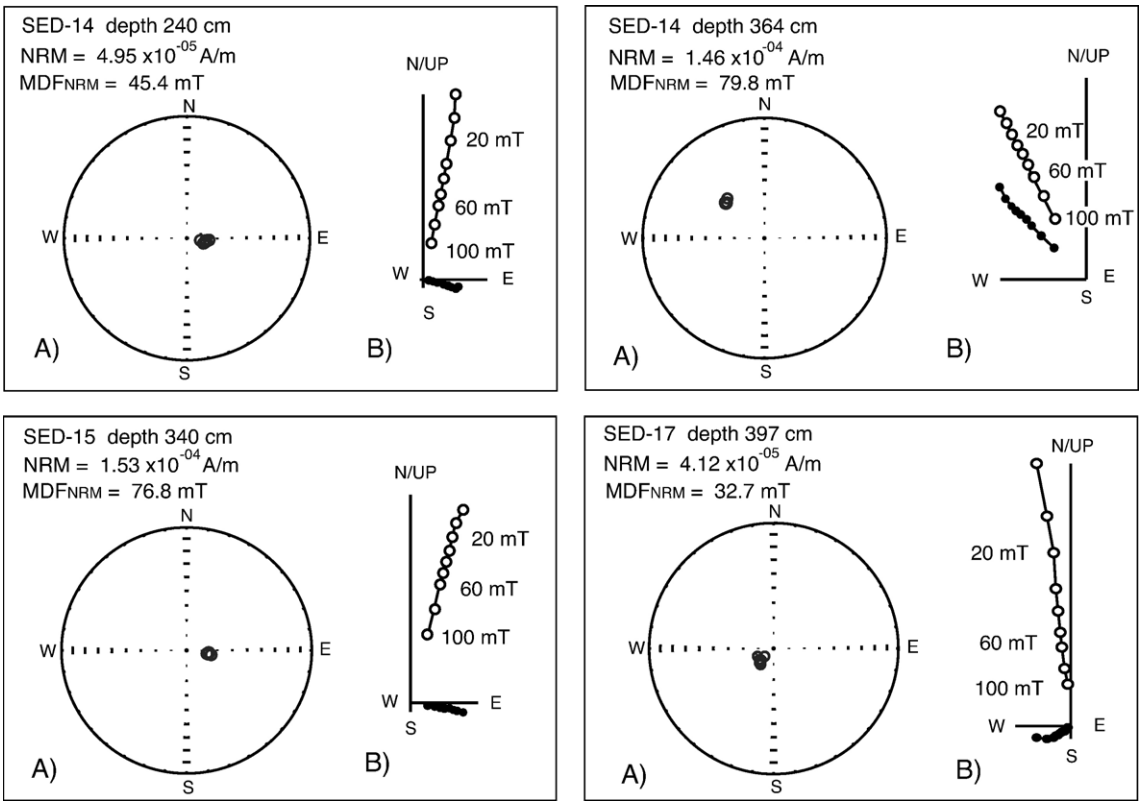

Fig. 2. Representative alternating field (AF) demagnetization plots for selected depths of the SEDANO cores. Paleomagnetic data indicated that the sediments carry a single-component natural remanent magnetization (NRM). A) Equal area projections: open symbols represent projection onto the upper hemisphere. B) Orthogonal vector diagrams: open (closed) circles represent projections on the vertical (horizontal) planes.

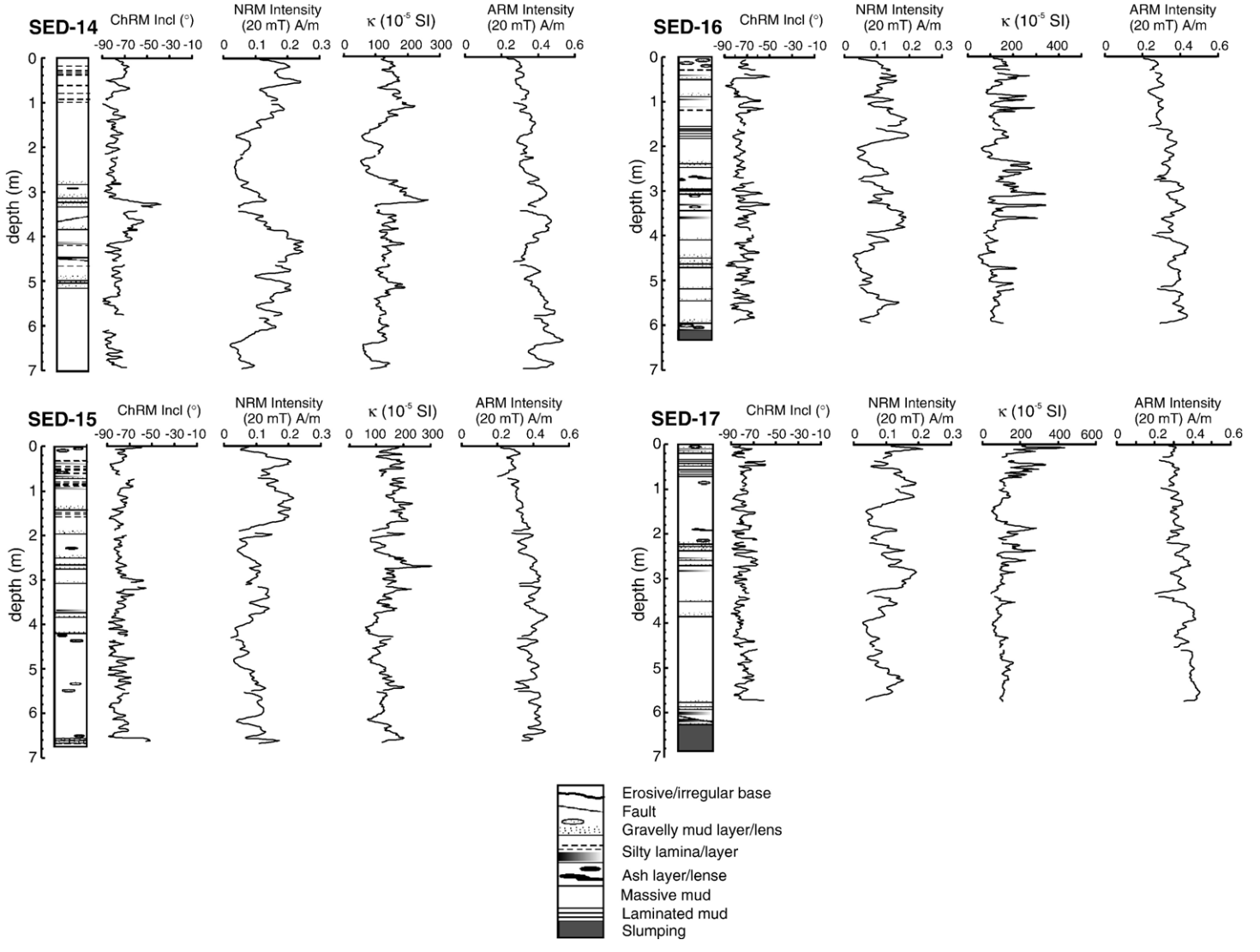

Fig. 3. Downcore variations of the characteristic remanent magnetization (ChRM) inclination, NRM, ARM (both after AF demagnetization at 20 mT) and κ intensities of the four SEDANO cores, plotted along the lithostratigraphic columns. For the lower part of SED-16 and SED-17 cores, characterized by unstable paleomagnetic behavior, no ChRM was isolated. The cores show always normal polarity, with ChRM inclination values oscillating around −78°, in agreement with the value expected at the high latitude of the sampling sites. Several swings to shallow inclination (up to values of −40°/−55°) are identified at different levels in the various cores. Stratigraphic trends of κ and ARM intensities indicate that variations in the abundance of magnetic particles are limited (see text for further explanations).

The NRM was progressively demagnetized by alternating field (AF) with peak values of 10–20–30–40–50–60–80–100 mT. Then an ARM was imparted by translating the u-channels in a constant symmetric AF of 100 mT with a superimposed direct current (DC) bias field of 0.1 mT, and subsequently stepwise demagnetized using the same sequence of AF peaks applied to the NRM. The translation speed of the u-channels through the AF coils, during the AF demagnetization treatment and the ARM acquisition procedure, was kept at 10 cm/s, that is the lowest speed allowed by the software running the measurements. This has effect on the efficiency of the AF demagnetization and the intensity of the produced ARM [52,53].

An IRM was also imparted on the u-channels in a steady DC field up to 0.9 T. However, as the intensity of the IRM exceeded the dynamic range of the SQUIDs, we will not take the IRM data on u-channel samples into account in the following.

Finally, with the aim of checking rock magnetic variations in the sedimentary sequence, hysteresis properties were measured on 17 chip specimens selected throughout core SED-16, using a MicroMag alternating gradient magnetometer (AGM, model 2900, Princeton Measurement Corporation) with a maximum applied field of 1 T. Hysteresis measurements were followed by the acquisition of an IRM and subsequent back-field demagnetization (both in a succession of fields up to 1 T, using the same AGM instrument).

4. NRM direction and paleointensity determinations

The characteristic remanent magnetization of the sediment (ChRM) was isolated by means of AF demagnetization (Fig. 2). Complete removal of any possible viscous component or magnetic overprint was achieved at low fields (10–20 mT). At higher AF the ChRM was identified as a single, stable and well defined remanence component, whose orientation was computed by principal component analysis [54] on the demagnetization steps.

Given that the NRM of the sediments is essentially a single-component remanence, from the stepwise AF demagnetization diagrams we derived the median destructive field of the NRM (MDF_{NRM}), defined as the field required to reduce the NRM intensity to one-half of its initial value. The MDF_{NRM} changes significantly throughout the cores (see examples in Fig. 2), with values mostly included in the range 40–80 mT. Only for the bottom parts of the SED-16 and SED-17 cores, both representing coarser slumping intervals, the NRM demagnetization diagrams did not allow a clear identification of a ChRM, due to unstable magnetic behavior. Consequently these two intervals were excluded from further interpretation.

Since the cores were oriented only with respect to the vertical, we will not discuss the results referring to the declination of the ChRM. However, the high latitude of the study site guarantees that the paleomagnetic inclination is representative enough of the paleomagnetic vectors and can provide unambiguous identification of the paleomagnetic polarity.

The ChRM indicates always normal magnetic polarity: the paleomagnetic inclination oscillates around a mean value of ca. −78° (−76.5°±7.8° for SED-14; −78.0°±6.0° for SED-15; −73.6°±6.6° for SED-16; −78.2°±7.7° for SED-17), in agreement with the value expected at ca. 67° S latitude.

The data show only a few thin intervals with anomalously shallow inclinations (from −40° to −55°) (Fig. 3). The lack of clear evidence for geomagnetic excursions, which are often reported in Brunhes sequences [see reviews in 13,37,55–57], may be due to the combined smoothing effects associated with the sedimentation rate, the acquisition of a post-depositional remanence (i.e. the unknown lock-in depth) [31,32], and the response functions of the SQUID sensors in the magnetometer [58,59]. The range of values for κ and ARM intensities through the stratigraphic sequences (50–500 10^{-5} SI and 0.2–0.5 A/m respectively) indicate variations within the same order of magnitude (Fig. 3), as well as for their mutual ratio ARM/κ. This indicates that the cores meet the magnetic uniformity criteria required for RPI studies [60,61].

Different normalization factors were proposed to obtain a reliable determination of the geomagnetic RPI from sedimentary sequences [i.e. 6,7,38,60–64]. Each normalization aims to remove the effect of variations in the concentration of the magnetic minerals carrying the ChRM.

In order to explore the effect of varying coercivities (as those indicated by the variable MDF_{NRM}), we divided NRM intensities measured at various steps of AF demagnetization by the ARM intensities measured at the same AF steps (Fig. 4A). Since the NRM high-coercivity fraction (that remained undemagnetized beyond 100 mT AF) was not affected by the ARM production in 100 mT AF, the ARM coercivity spectra is quite different from the NRM spectra and the NRM/ARM curves tend to diverge in AF higher than 50–60 mT. On the other hand, the NRM/ARM curves keep the same trend using the NRM intensity at various AF steps and a constant normalizing ARM intensity at low AF values (i.e. after 20 mT AF; see Fig. 4B).

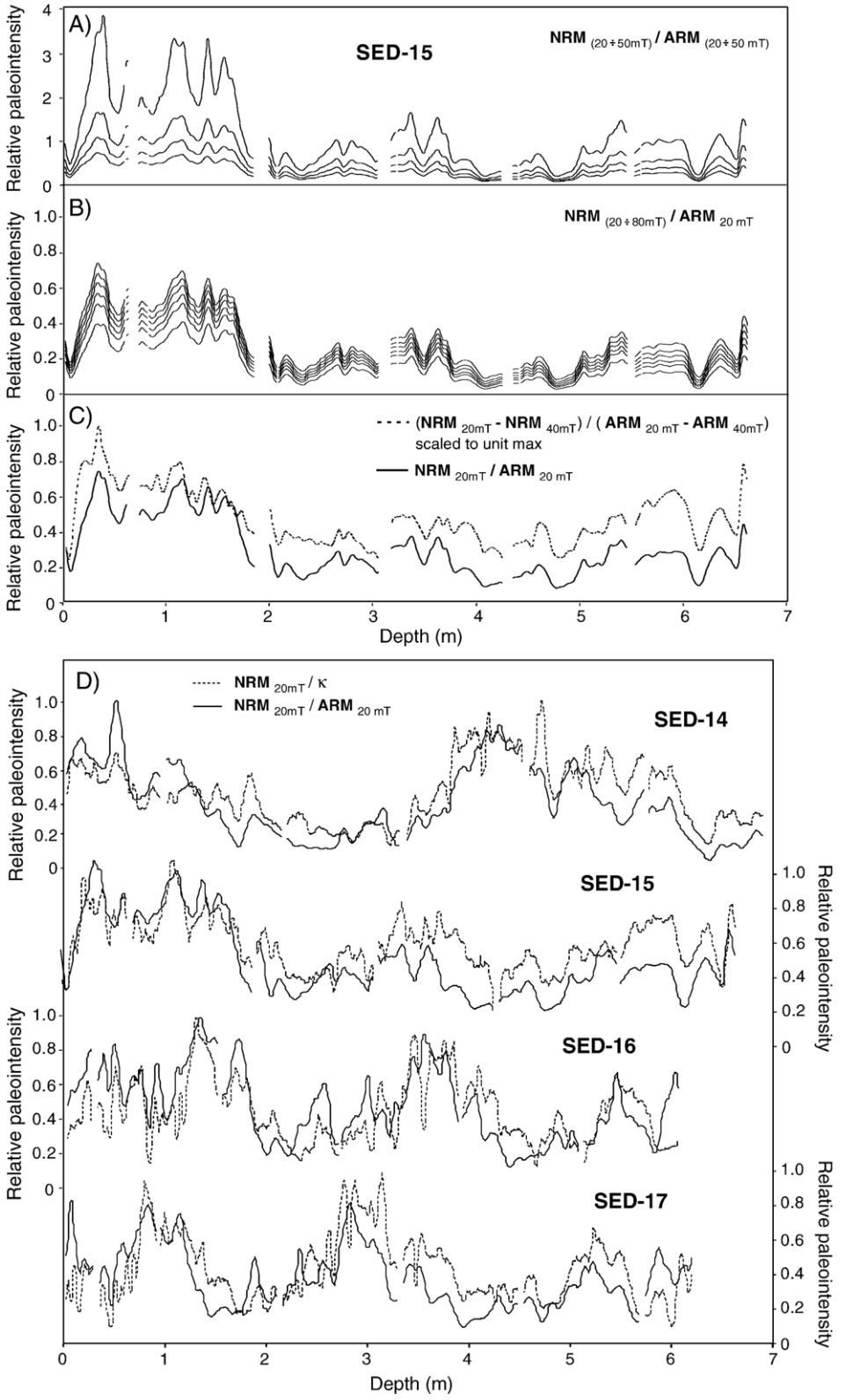
A)
SED-15
NRM (20÷50mT) / ARM (20÷50 mT)
B)
NRM (20÷80mT) / ARM 20 mT
C)
(NRM 20mT - NRM 40mT) / (ARM 20 mT - ARM 40mT)
scaled to unit max
NRM 20mT / ARM 20 mT
Relative paleointensity
Depth (m)
D)
NRM 20mT / κ
NRM 20mT / ARM 20 mT
SED-14
SED-15
SED-16
SED-17
Relative paleointensity
Depth (m)

We also computed a normalized curve using the subtracted vector method [i.e., 38] ($NRM_{20\,mT} - NRM_{40\,mT}$)/($ARM_{20\,mT} - ARM_{40\,mT}$), in which the high-coercivity component is removed from the equation (Fig. 4C). This normalization provided essentially the same trend observed with the "classic" normalization techniques that make use of the whole vectors (Fig. 4B). We assumed that the fraction with coercivity in the range 20–40 mT is the more reliable recorder of past RPI variation. Therefore, in this study we selected the RPI records obtained by dividing the NRM intensity, demagnetized at 20 mT ($NRM_{20\,mT}$), by κ and the ARM intensity after demagnetization at 20 mT ($ARM_{20\,mT}$) (Fig. 4D).

For each core, the two normalized RPI records ($NRM_{20\,mT}/\kappa$ and $NRM_{20\,mT}/ARM_{20\,mT}$) do not differ very much from bulk NRM trends and show mostly similar stratigraphic patterns (Fig. 4D). Nevertheless, since the presence of sparse pebbles or slightly coarser grained intervals at various stratigraphic heights induces sharp peaks in the magnetic susceptibility records, but does not significantly affect natural and anhysteretic remanence intensities, the $ARM_{20\,mT}$ seems to be the more appropriate normalization parameter.

5. Correlation of RPI records and chronology of the sequences

Following the establishment of worldwide RPI reference stacks [14,15], records of geomagnetic paleointensity variation can be used to develop original high-resolution age models in sedimentary sequences, which are especially important when the use of more traditional chronostratigraphic proxy is limited, as for the Antarctic sediments discussed here.

The normalized records $NRM_{20\,mT}/ARM_{20\,mT}$ obtained for the SEDANO cores have been correlated with the SINT-800 reference paleointensity curve [15] (Fig. 5), in order to improve the former age model available for the sedimentary sequence [41,43]. We used the Analyseries 1.2 software of Paillard et al. [65], that allows adjustment and correlation between selected pairs of depth-age tie points of two numerical series, to transfer SINT-800 RPI ages to the individual SEDANO RPI records. RPI curves were thus matched on the basis of the visual correlation of the main paleointensity features: RPI lows occur at 38–40 ka, around 65 ka, at 95–125 ka, and at ca. 190 ka. RPI highs occur at 55 ka, at 70–80 ka, at 160–170 ka, around 230 ka and at 255 ka.

The developed RPI age models indicate that the SED-14 core spans the interval from ca. 28 to 205 kyr, both SED-15 and SED-16 cores extend up to about

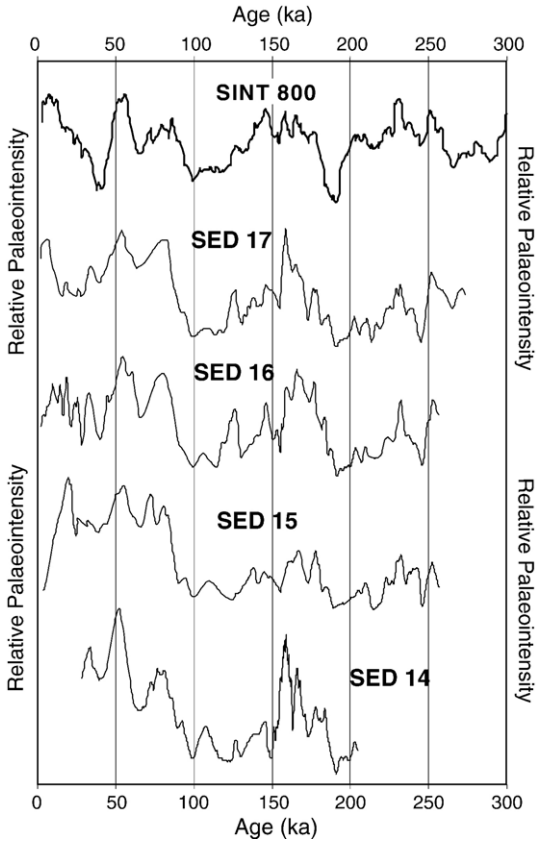

Fig. 5. The relative paleointensity (RPI) records ($NRM_{20\,mT}/ARM_{20\,mT}$) obtained for each of the SEDANO cores are compared to the SINT-800 reference curve of Guyodo and Valet [1]. The RPI curves can be matched by identification of common features with periods longer than a few kyr, providing an original age model for the sedimentary sequences. The results indicate that the cores span an age interval back to ca. 270 kyr.

Fig. 4. NRM/ARM ratios for the SED-15 core: A) after AF demagnetization of both parameters at steps of 20, 30, 40 and 50 mT; B) after demagnetization of NRM at different AF steps (20–80 mT) and ARM demagnetized at 20 mT AF only; C) using the subtracted vector method in the low-coercivity range ($NRM_{20\,mT} - NRM_{40\,mT}$)/($ARM_{20\,mT} - ARM_{40\,mT}$), in order to exclude the contribution of the high-coercivity component in the normalized curves. D) Normalized NRM intensity curves ($NRM_{20\,mT}/\kappa$ and $NRM_{20\,mT}/ARM_{20\,mT}$) for all the studied SEDANO cores. Both curves show a similar pattern at low frequencies with discrepancies in correspondence of pebbles and/or silty levels in the cores. For the lower part of SED-16 and SED-17 cores, a coarser slump characterized by unstable paleomagnetic behavior, NRM intensity curve was not computed. Lithostratigraphic logs and symbols as in Fig. 3.

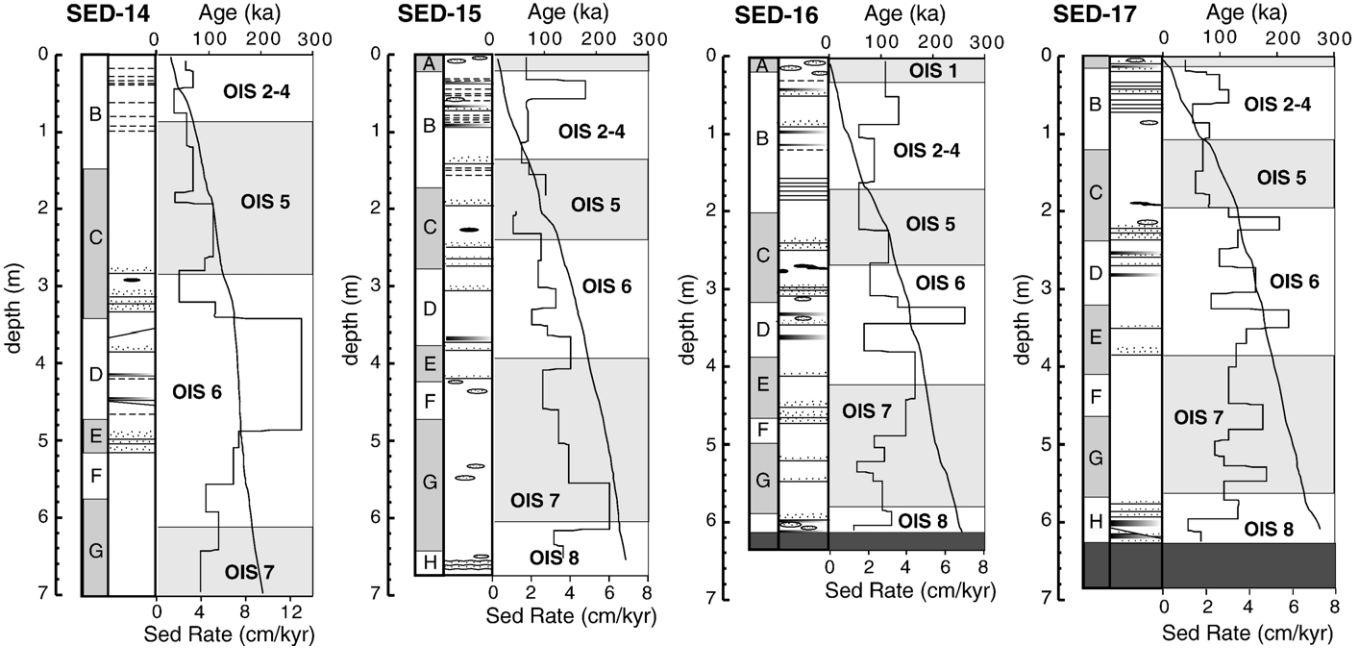

Fig. 6. Downcore variation of the sedimentation rates estimated by the new RPI age model. Lithostratigraphic logs and symbols as in Fig. 3. Unbroken line: age versus depth; broken line: age versus sedimentation rate calculated between the RPI tie points. The grey (white) areas indicate interglacial (glacial) intervals (OIS = oxygen isotope stages, with ages of stages transitions derived from Bassinot et al. [21]). In the plots, position of glacial and interglacial intervals was determined from the estimated RPI chronology, whereas in the thin columns to the left of the lithostratigraphic logs their position is placed according to the previous age model of Lucchi et al. [41], with estimated glacial–interglacial periods indicated with capital letters A–H.

257 kyr, while the SED-17 core spans the last 274 kyr (Fig. 5).

The detailed age models reconstructed by means of RPI data allowed to estimate the variation of sedimentation rate among the different cores and through the stratigraphic sequence of each core (Fig. 6). The mean sedimentation rates are similar (ca. 2.3 cm/kyr) for the SED-14, SED-15 and SED-16 cores, and just a little reduced for the SED-17 core placed in a more distal position towards the abyssal plain (ca. 1.9 cm/kyr) (see Fig. 1). The main changes in the sedimentation rates between the tie points generally correspond to lithological variations or to breaks between consecutive u-channels.

The reconstructed sedimentation rates, when compared to those computed at more proximal sites in Drift 7 (varying in the range 2–10 cm/kyr for cores SED-02; SED-04 and SED-06 [34]), indicate a progressive decrease in the sedimentation rate moving away from the continental slope.

Before the present study, the age model for the SEDANO cores was mostly built on lithostratigraphic models, without the support of radiometric dating and carbon or oxygen stable isotopes, and supposed to span through OIS 1 to OIS 11 [41,43,44]. Our RPI chronology is in reasonable agreement with the previous age model of Lucchi et al. [41] up to the interglacial C, corresponding to the OIS 5 (Fig. 6), and assigns an age of 125–129 ka to the tephra layer recognized in each of the SEDANO cores at the bottom of the interglacial unit C, that is in agreement with the age of a 11-cm thick ash layer found in the EPICA-Dome C ice cores and dated at 129.5 ka [46,47].

For the older core section, however, remarkable differences were found with former age model, suggesting that the cores are younger than previously supposed and limited to OIS 8, and indicating a new, detailed, correlation of stratigraphic intervals to glacial–interglacial cycles (Fig. 6).

6. Environmental magnetism

The study of variable rock magnetic records in a sedimentary sequence is recognized as a powerful tool to trace and quantify environmental changes, and the environmental magnetism is now a well established discipline [66–71]. In this perspective, the downcore variations of the magnetic properties in a sedimentary sequence could reflect changes in the composition, concentration and grain size of magnetic minerals. Low-field magnetic susceptibility (κ) and anhysteretic remanent magnetization (ARM) are generally indicative of the concentration of ferrimagnetic minerals [66,68,72–74], while the ARM/κ ratio is a proxy for grain size variations of ferrimagnetic particles [60,72,75]. The median destructive field of natural remanence (MDF_{NRM}), in case of a single NRM component, represents a useful parameter to estimate the coercivity of the remanence carriers and may be diagnostic of the magnetic mineralogy [34,66,68].

The MDF_{NRM} may also depend on magnetic viscosity, since a sample with large viscosity has a lower MDF_{NRM} than a non-viscous sample. Anyway, in our case the presence of a viscous component is almost negligible (see Fig. 2) and the correlation of the MDF_{NRM} values with the coercivity values estimated from hysteresis measurements on selected chip specimens from core SED-16 (Fig. 7) demonstrate that the MDF_{NRM} directly depends on factors related to magnetic mineralogy.

Sagnotti et al. [34] suggested that the magnetic mineralogy of the SEDANO cores reflects a variable proportion in the mixture of magnetic minerals with varying coercivities, carrying the same ChRM. Whereas the low-coercivity phase can be identified as magnetite, by rock magnetic data, magnetic iron sulfides were proposed as the most likely candidates for the fraction with higher coercivities [34]. Variation in the MDF_{NRM} values of the SEDANO cores should therefore depend on the variable proportion of low- and intermediate-coercivity phases.

The stratigraphic variations of the main magnetic parameters measured for each SEDANO core (κ, ARM, ARM/κ MDF_{nrm} and MDF_{arm}) are in good agreement (Fig. 8) and consistent with the boundaries of interglacial and glacial periods (according to the chronology of Bassinot et al. [21]) as deduced from our RPI chronology (see also Fig. 6). The $ARM_{20\ mT}$ intensity shows limited downcore oscillations, as well as κ, indicating a substantial uniformity in the overall magnetic mineral concentration.

Within this range of variation, no clear correlation is observed between alternating intervals of high and low magnetic mineral concentration, or magnetic grain size, and the glacial–interglacial cycles. This concurs with the inference that along the individual cores the average sediment accumulation rates do not show substantial differences throughout the glacial–interglacial intervals.

On the other hand, high frequency variations are recognized for the ARM/κ ratio, with features that may be correlated between the cores and maximum peaks corresponding to minimum values in the MDF_{NRM} parameter (Fig. 8). The latter shows the more pronounced, and clear, rock magnetic variations in the SEDANO cores.

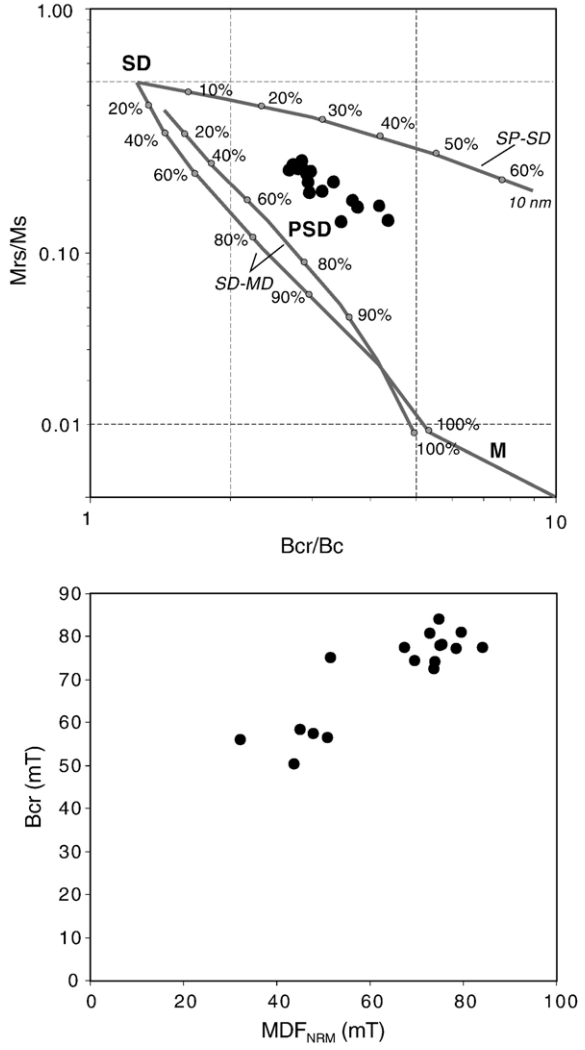

Fig. 7. A) Plot of hysteresis ratios (B_{CR}/B_C vs M_{RS}/M_S; after [79]) for 17 selected specimens from core SED-16, with variable median destructive field of the natural remanence (MDF_{NRM}). B_{CR}: remanent coercive force, B_C: coercive force, M_{RS}: saturation remanent magnetization; M_S: saturation magnetization. Fields for single domain (SD), pseudo single domain (PSD) and multidomain (MD) (titano) magnetite grains and the theoretical lines for mixtures of single domain (SD) and multidomain (MD) grains and of SD and superparamagnetic (SP) grains are shown according to Dunlop [80]. B) Plot of B_{CR} vs MDF_{NRM} for the same 17 selected specimens. The hysteresis data are compatible with a mixture of different magnetic particles and indicate that MDF_{NRM} is correlated to coercivity.

In fact, MDF_{NRM} is distinctly lower during the interglacial periods (with minimum values of 35–40 mT) and constantly higher (up to ca. 80 mT) during the glacial periods. This trend was already noted on cores SED-02, SED-04 and SED-06, spanning the last 160 kyr, in Drift 7 [34]. The median destructive field of the ARM (MDF_{arm}) oscillates in the narrow range of 25–30 mT, confirming that the ARM was only acquired by the low-coercivity fraction, identified with magnetite [34].

The new age model allowed to document that the concentration of the higher coercivity phase decreases systematically (for three full consecutive glacial–interglacial cycles) during interglacial intervals, resulting in a drop of the MDF_{NRM} toward values typical for magnetite (about 40 mT; see Fig. 8). The inference that some of the rock magnetic variations are climatically-driven is supported by the observation that low MDF_{NRM} and κ values, when plotted versus age (as derived from RPI), correlate to negative $\delta^{18}O$ values of the SPECMAP oxygen isotope stack [19] (Fig. 9). We argue that the alternation of climatic periods induced only a disproportion on the relative abundance of two distinct magnetic mineral populations at the SEDANO cores location, whereas lithology, sedimentation rates and other rock magnetic parameters are barely affected by climatic changes. Such disproportion essentially results from variation in the abundance of the magnetic phase with higher coercivity.

If identification of this phase with early authigenic ferrimagnetic iron sulfides is correct [34], this implies that climatic changes induced local changes in the redox conditions or in the availability of detrital organic matter, which are the major controlling factors on the pyritization process and may result in the preservation of intermediate magnetic iron sulfides [76–78].

According to Lucchi and Rebesco [41], the preservation of laminae and the lack of bioturbation in SEDANO glacial sediments may be linked to a permanent sea-ice extension over the area during glacial periods, inducing a reduction in primary productivity, absence of biological activity at the sea bottom and oxygen-reduced deep waters. These conditions are in fact favorable to the preservation of intermediate magnetic iron sulfides.

7. A stacked paleointensity record for the SEDANO cores

The individual normalized RPI records were merged in a SEDANO RPI stacking curve spanning the last 270 kyr and compared to the SINT-800 RPI stack [15] (Fig. 10).

The RPI stacked curve was computed from the estimated age model for the individual SEDANO RPI records: the arithmetic mean and the standard deviation of all the scaled $NRM_{20\ mT}/ARM_{20\ mT}$ values were computed at 1 kyr spacing, using all values with an assigned age included in a range of ±500 yr

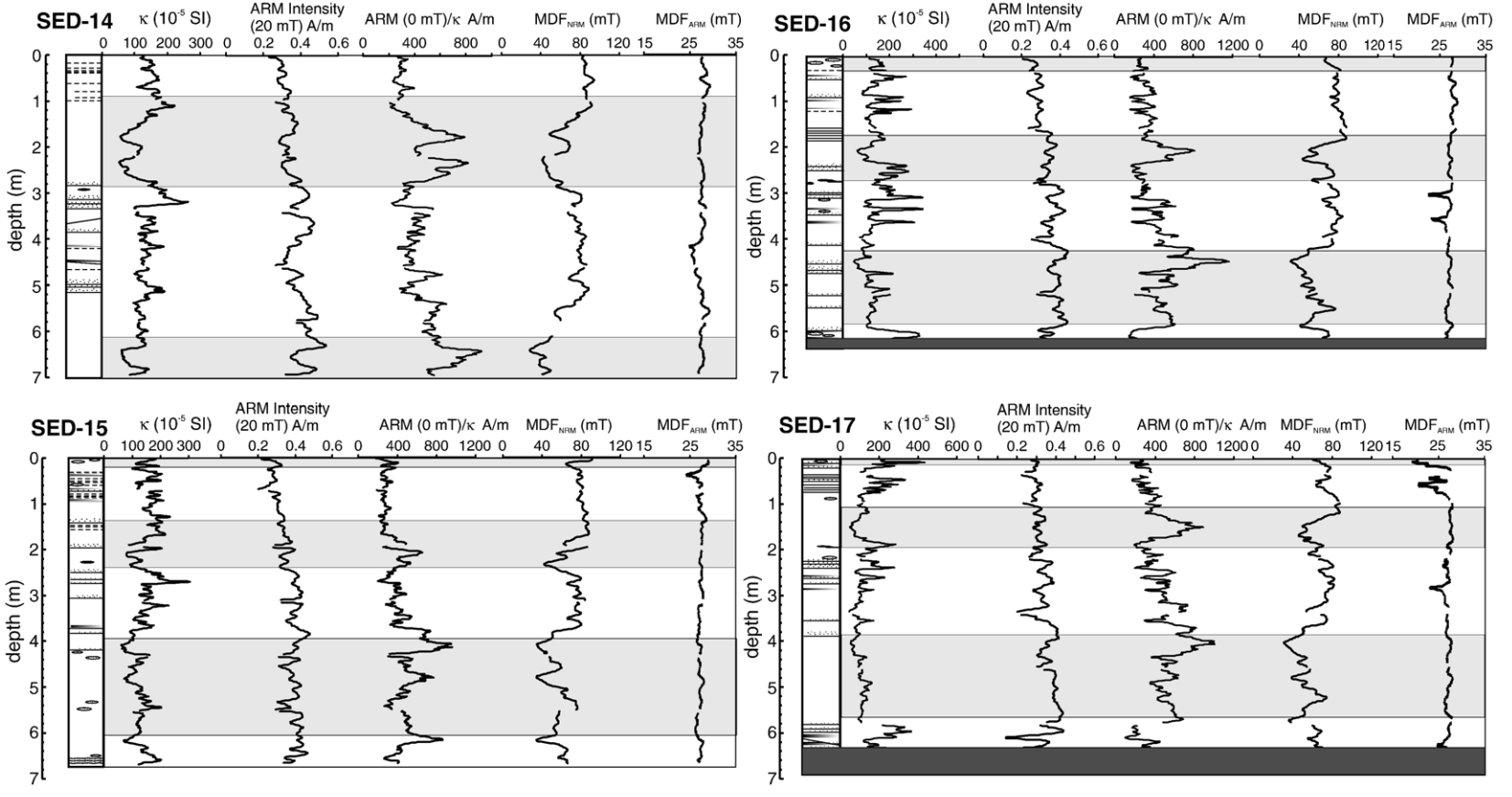

Fig. 8. Downcore variation of the main rock magnetic parameters measured for each cores (κ, ARM, ARM/κ, MDF_{NRM}, MDF_{arm}). The grey (white) areas indicate interglacial (glacial) intervals (with ages of climatic stages transitions derived from Bassinot et al. [21]). The rock magnetic parameters appear almost not significantly affected by the alternation of climatic periods. The main influence of climatic changes is recognized for the MDF_{NRM} values, with values during glacial periods constantly higher (and less variable) than in interglacials. Minima in MDF_{NRM} values correspond to maxima in ARM/κ (see text for discussion).

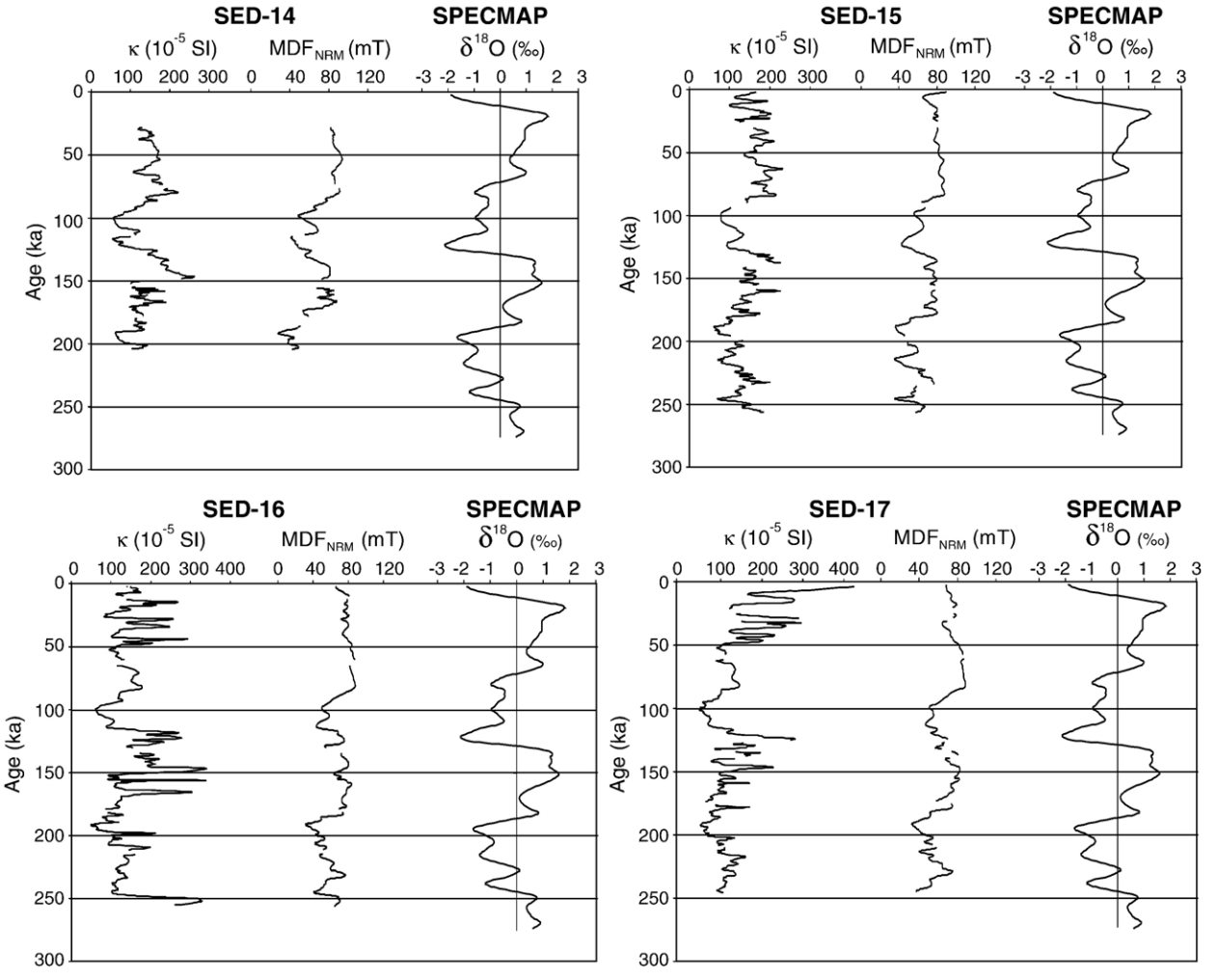

Fig. 9. κ and MDF_{nrm} parameters plotted versus age (based on the new RPI chronology) and compared to the SPECMAP orbitally tuned $\delta^{18}O$ reference curve [19]. The oxygen isotope records and the rock magnetic parameters appear optimally correlated, with minima in the selected rock magnetic parameters occurring during interglacial stages.

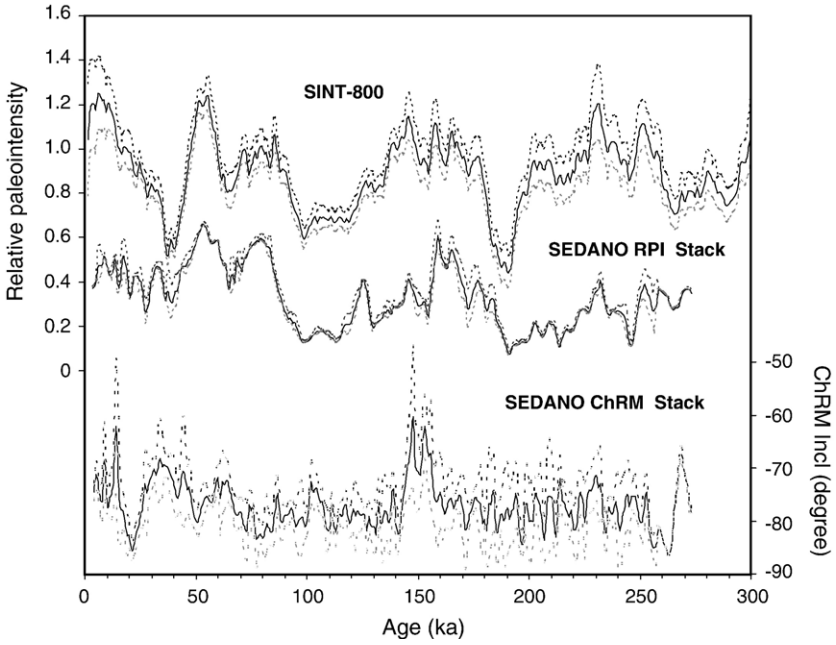

Fig. 10. The RPI stacking curve for the SEDANO cores, compared to the SINT-800 reference curve of Guyodo and Valet [1], with dashed lines indicating the standard deviation. The SINT-800 curve is scaled by unit mean, whereas, for graphical comparison, the SEDANO RPI stack was scaled to unit maximum.

centered on each incremental 1 kyr age step. The SINT-800 and the SEDANO RPI stacks share common features with periods longer than a few to 10 kyr (Fig. 10).

The standard deviation computed for the SEDANO stack is generally smaller than that associated with the SINT-800, indicating a remarkably good coherence between the individual SEDANO RPI curves. We recognize, however, that a proper interpretation of the sedimentary record in terms of high-frequency geomagnetic field variations should take into account the smoothing effects due to multiple sources, such as those due to measurement and dating of core samples (for comprehensive reviews see [33,59]).

The stack of the ChRM inclination records (Fig. 9) shows only two intervals with anomalously shallow paleomagnetic inclinations (with values up to −60°), and larger standard deviation, that are however not correlated to any known paleomagnetic excursion.

The youngest interval is short and centered at ca. 14 ka and mostly results from record of the SED-16 core (Fig. 3). The older interval, dated at ca. 140–160 ka, mostly results from the record of the SED-14 core (Fig. 3). Both intervals are associated to slightly coarser lithologies and may be due to uncompensated lithological effects. We note that coarser lithologies may affect the fidelity with which paleomagnetic inclination and RPI are recorded and may be the cause of the discrepancies between the SEDANO RPI stack and the SINT-800 observed at about 150 ka and also of the shallow paleomagnetic inclinations observed for the same time interval.

A difference between the SEDANO RPI stack and the SINT-800 is also evident in the younger part of the record and may be due to sampling disturbance at the top of the cores. Anyway, we note that the rather uniform rise in RPI values reported for the SINT-800 between 40 and 10 ka was not observed in various other RPI records from northern and southern high latitudes [12,16–18,34,37]. Moreover, we recognize that the natural sedimentary smoothing of the primary geomagnetic signal, due to the sedimentation rate and the lock-in process, and the response function of the pick-up coils in the magnetometer, can affect the ability of a sedimentary sequence to record transient geomagnetic features [31,33,59]. Therefore, the lack of clear evidence of geomagnetic excursions in the SEDANO cores may be due to a combination of relatively low sedimentation rate and various natural and instrumental smoothing effects.

8. Conclusions

Paleomagnetic and rock magnetic studies conducted on the SEDANO cores allowed to construct RPI

records that were dated by correlation to the RPI global stack curve SINT-800 [15].

The individual normalized RPI records were merged in a SEDANO RPI stack record, that provides a high-resolution image of the geomagnetic field variation at the southern high latitudes, spanning the last 270 kyr. Geomagnetic relative paleointensity can serve as a regional tool for high-resolution correlation and dating of other coeval sedimentary sequences from the peri-Antarctic margins.

The proposed RPI chronology, supported by several lithostratigraphic constraints and by climatically-driven rock magnetic variations, establish that all the SEDANO cores are Late Pleistocene in age, but younger than formerly supposed, reaching back to OIS 8. The detailed RPI age models also allowed to estimate at about 2 cm/kyr the mean sedimentation rates for the four studied cores and indicate a progressive reduction of the sedimentation rate on the Drift 7, moving away from the continental slope.

We propose an original, high-resolution, correlation of stratigraphic intervals to glacial–interglacial cycles, providing new constraints to assess ages, rates and amplitudes of the climatic and environmental changes affecting this key area of the peri-Antarctic margins during the Late Pleistocene. In fact, lithology and the overall rock magnetic characters suggest that environmental variations at the SEDANO sites were rather limited, yet recognizable, during the last three glacial–interglacial cycles. The rock magnetism indicates that the main variations driven from climatic alternations were observed for the coercivity dependent MDF_{nrm} parameter, with relatively high values (about 80 mT) during the glacial periods and relatively lower values (about 40 mT) during the interglacials. The MDF_{nrm} trend suggests changes in the relative proportion of two magnetic mineral populations with distinct coercivities and point out that magnetic coercivity is a valid proxy of paleoenvironmental changes in these sedimentary Drift sequences. Under the assumption that the intermediate-coercivity magnetic phase is represented by early authigenic magnetic iron sulfides [34], the climatically-driven changes at the SEDANO sites involved mostly variations in the redox conditions or in the input of decomposable organic matter.

The environmental variability reconstructed for the SEDANO cores contrasts with observations from similar coeval records from the Wilkes Land margin, which indicate a substantial uniformity during the Late Pleistocene glacial–interglacial cycles [37]. The difference between the two sectors corroborate the inference of a general higher stability of the East Antarctic ice sheet with respect to the Western Antarctic ice sheet, and the Antarctic Peninsula in particular, during the climatic cycles of Late Pleistocene.

Acknowledgments

The SEDANO (SEdiment Drifts of the ANtarctic Offshore) program has been funded by PNRA (*Programma Nazionale di Ricerche in Antartide*). All the members of the SEDANO working group provided fundamental help with continued discussion on cores stratigraphy and sedimentology.

In particular we are pleased to acknowledge Claus-D Hillenbrand for the useful comments on the tephra chronology, Andrea Caburlotto for the technical assistance during the sampling work and Gianguido Salvi from *Museo Nazionale dell'Antartide* of Trieste for the logistical support. The manuscript was greatly improved by constructive comments of J.-P. Valet and an anonymous reviewer.

References

[1] D.V. Kent, N.D. Opdyke, Paleomagnetic field intensity variation recorded in a Brunhes epoch deep-sea sediment core, Nature 266 (1977) 156–159.

[2] L. Tauxe, J.P. Valet, Relative paleointensity of the Earth's magnetic field from marine sedimentary cores: a global perspective, Phys. Earth Planet. Inter. 56 (1989) 59–68.

[3] L. Tauxe, G. Wu, Normalized remanence in sediments of the western equatorial Pacific: relative paleointensity of the geomagnetic field? J. Geophys. Res. 95 (1990) 12337–12350.

[4] L. Tauxe, N.J. Shackleton, Relative paleointensity records from the Ontong–Java Plateau, Geophys. J. Int. 117 (1994) 769–782.

[5] L. Meynadier, J.P. Valet, R. Weeks, N.J. Shackleton, V.L. Hagee, Relative geomagnetic intensity of the field during the last 140 ka, Earth Planet. Sci. Lett. 114 (1992) 39–57.

[6] E. Tric, J.P. Valet, P. Tucholka, M. Parterne, L. Labeyrie, F. Guichard, L. Tauxe, M. Fontune, Paleointensity of the geomagnetic field during the last eighty thousand years, J. Geophys. Res. 97 (1992) 9337–9351.

[7] J.S. Stoner, J.E.T. Channell, C. Hillaire-Marcel, A 200 ka geomagnetic chronostratigraphy for the Labrador Sea: indirect correlation of the sediment record to SPECMAP, Earth Planet. Sci. Lett. 159 (1998) 165–181.

[8] J.-P. Valet, L. Meynadier, F.C. Bassinot, F. Garnier, Relative paleointensity across the last geomagnetic reversal from sediments of the Atlantic, Indian and Pacific Oceans, Geophys. Res. Lett. 21 (1994) 485–488.

[9] T. Yamazaki, Relative paleointensity of the geomagnetic field during Brunhes Chron recorded in North Pacific deep-sea sediment cores: orbital influence? Earth Planet. Sci. Lett. 169 (1999) 23–35.

[10] J.E.T. Channell, D.A. Hodell, B. Lehman, Relative geomagnetic paleointensity and $\delta^{18}O$ at ODP Site 983 (Gardar Drift, North Atlantic) since 350 ka, Earth Planet. Sci. Lett. 153 (1997) 103–118.

[11] J.E.T. Channell, J.S. Stoner, D.A. Hodell, C.D. Charles, Geomagnetic paleointensity for the last 100 kyr from the sub-

antarctic South Atlantic: a tool for inter-hemispheric correlation, Earth Planet. Sci. Lett. 175 (2000) 145–160.
[12] J.E.T. Channell, Geomagnetic paleointensity and directional secular variation at Ocean Drilling Program (ODP) site 984 (Bjorn Drift) since 500 ka: comparisons with ODP site 983 (Gardar drift), J. Geophys. Res. 104 (1999) 22937–22951.
[13] N. Thouveny, J. Carcaillet, E. Moreno, G. Leduc, D. Nerini, Geomagnetic moment variation and paleomagnetic excursions since 400 kyr BP: a stacked record from sedimentary sequences of the Portuguese margin, Earth Planet. Sci. Lett. 219 (2004) 377–396.
[14] Y. Guyodo, J.-P. Valet, Relative variations in geomagnetic intensity from sedimentary records: the past 200.000 years, Earth Planet. Sci. Lett. 143 (1996) 23–36.
[15] Y. Guyodo, J.-P. Valet, Global changes in intensity of the Earth's magnetic field during the past 800 kyr, Nature 399 (1999) 249–252.
[16] C. Laj, C. Kissel, A. Mazaud, J.E.T. Channell, J. Beer, North Atlantic paleointensity stack since 75 ka (NAPIS-75) and the duration of the Laschamp event, Philos. Trans. R. Soc. Lond. A-358 (2000) 1009–1025.
[17] J.S. Stoner, C. Laj, J.E.T. Channell, C. Kissel, South Atlantic (SAPIS) and North Atlantic (NAPIS) geomagnetic paleointensity stacks (0–80 ka): implications for inter-hemispheric correlation, Quat. Sci. Rev. 21 (2002) 1141–1151.
[18] C. Laj, C. Kissel, J. Beer, High resolution global paleointensity stack since 75 kyr (GLOPIS-75) calibrated to absolute values, Timescales of the Paleomagnetic field, AGU Geophysical Monograph Series, vol. 145, 2004, pp. 255–265.
[19] J. Imbrie, J.D. Hays, D.G. Martinson, A. McIntyre, A.C. Mix, J.J. Morley, N.G. Pisias, W.L. Prell, N.J. Shackleton, The orbital theory of Pleistocene climate: support from a revised chronology of the marine $\delta^{18}O$ record, in: A. Berger, J. Imbrie, J. Hays, G. Kukla, B. Saltzman (Eds.), Milankovitch and Climate (Pt. 1), NATO ASI Ser. C, Math Phys. Sci., vol. 126, 1984, pp. 269–305.
[20] D.G. Martinson, N.G. Pisias, J.D. Hays, J. Imbrie, T.C. Moore, N.J. Shackleton, Age dating and the orbital theory of the ice ages: development of a high-resolution 0 to 300,000-year chronostratigraphy, Quat. Res. 27 (1987) 1–19.
[21] F.C. Bassinot, L.D. Labeyrie, E. Vincent, X. Quidelleur, N.J. Shackleton, Y. Lancelot, The astronomical theory of climate and the age of the Brunhes–Matuyama reversal, Earth Planet. Sci. Lett. 126 (1994) 91–108.
[22] D.V. Kent, D.A. Schneider, Correlation of paleointensity variation records in the Brunhes/Matuyama polarity transition interval, Earth Planet. Sci. Lett. 129 (1995) 135–144.
[23] P. Hartl, L. Tauxe, A pre-cursor to the Matuyama/Brunhes transition-field instability as recorded in pelagic sediments, Earth Planet. Sci. Lett. 138 (1996) 121–136.
[24] C. Laj, C. Kissel, F. Garnier, E. Herrero-Bervera, Relative geomagnetic field intensity and reversals for the last 1.8 My from a central equatorial Pacific core, Geophys. Res. Lett. 23 (1996) 3393–3396.
[25] K.L. Verosub, E. Herrero-Bervera, A.P. Roberts, Relative geomagnetic paleointensity across the Jaramillo subchron and the Matuyama/Brunhes boundary, Geophys. Res. Lett. 23 (1996) 467–470.
[26] Y.S. Kok, L. Tauxe, A relative geomagnetic paleointensity stack from Ontong–Java Plateau sediments for the Matuyama, J. Geophys. Res. 104 (1999) 25401–25413.
[27] Y. Guyodo, G.D. Acton, S. Brachfeld, J.E.T. Channell, A sedimentary paleomagnetic record of the Matuyama Chron from the western Antarctic margin (ODP Site 1101), Earth Planet. Sci. Lett. 191 (2001) 61–74.
[28] J. Dinarès-Turell, L. Sagnotti, A.P. Roberts, Relative geomagnetic paleointensity from the Jaramillo subchron to the Matuyama/Brunhes boundary as recorded in a Mediterranean piston core, Earth Planet. Sci. Lett. 194 (2002) 327–341.
[29] C.-S. Horng, A.P. Roberts, W.-T. Liang, A 2.14-Myr astronomically tuned record of relative geomagnetic paleointensity from the western Philippine Sea, J. Geophys. Res. 108 (2003) 2059, doi:10.1029/2001JB001698.
[30] T. Yamazaki, H. Oda, A geomagnetic paleointensity stack between 0.8 and 3.0 Ma from equatorial Pacific sediment cores, Geochem. Geophys. Geosyst. 4 (2005), doi:10.1029/2005GC001001.
[31] A.P. Roberts, M. Winklhofer, Why are geomagnetic excursions not always recorded in sediments? Constraints from post-depositional remanent magnetization lock-in modeling, Earth Planet. Sci. Lett. 227 (3–4) (2004) 345–359.
[32] L. Sagnotti, F. Budillon, J. Dinarès-Turell, M. Iorio, P. Macrì, Evidence for a variable paleomagnetic lock-in depth in the Holocene sequence from the Salerno Gulf (Italy): implications for "high-resolution" paleomagnetic dating, Geochem. Geophys. Geosyst. 6 (11) (2005), doi:10.1029/2005GC001043.
[33] D.G. McMillan, C.G. Constable, R.L. Parker, Assessing the dipolar signal in stacked paleointensity records using a statistical error model and geodynamo simulations, Phys. Earth Planet. Inter. 145 (2004) 37–54.
[34] L. Sagnotti, P. Macrì, A. Camerlenghi, M. Rebesco, Environmental magnetism of late Pleistocene sediments from the pacific margin of the Antarctic Peninsula and interhemispheric correlation of climatic events, Earth Planet. Sci. Lett. 192 (2001) 65–80.
[35] S.A. Brachfeld, G.D. Acton, Y. Guyodo, S.K. Banerjee, High-resolution paleomagnetic records from Holocene sediments from the Palmer Deep, western Antarctic Peninsula, Earth Planet. Sci. Lett. 181 (2000) 421–441.
[36] S.A. Brachfeld, E.W. Domack, C. Kissel, C. Laj, A. Leventer, S.E. Ishman, R. Gilbert, A. Camerlenghi, L.B. Eglinton, Holocene history of the Larsen ice shelf constrained by geomagnetic paleointensity dating, Geology 31 (2003) 749–752.
[37] P. Macrì, L. Sagnotti, J. Dinarès-Turell, A. Caburlotto, A composite record of late Pleistocene relative geomagnetic paleointensity from the Wilkes Land Basin (Antarctica), Phys. Earth Planet. Inter. 151 (2005) 223–242.
[38] J.S. Stoner, J.E.T., D.A. Hodell, C.D. Charles, A ~580 kyr paleomagnetic record from the sub-Antarctic South Atlantic (Ocean Drlling Program Site 1089), J. Geophys. Res. 108 (B5) (2003) 2244, doi:10.1029/2001JB001390.
[39] M. Rebesco, R.D. Larter, A. Camerlenghi, P.F. Barker, Giant sediment drifts on the continental rise west of the Antarctic Peninsula, Geo Mar. Lett. 16 (1996) 65–75.
[40] M. Rebesco, R.D. Larter, P.F. Barker, A. Camerlenghi, L.E. Vanneste, The history of sedimentation on the continental rise west of the Antarctic Peninsula, Am. Geophys. Union Antarct. Res. Ser. 71 (1997) 29–49.
[41] G.R. Lucchi, M. Rebesco, A. Camerlenghi, M. Busetti, L. Tomadin, G. Villa, D. Persico, C. Morigi, M.C. Bonci, G. Giorgetti, Mid-late Pleistocene glacimarine sedimentary processes of a high-latitude deep-sea sediment drift (Antarctic Peninsula margin), Mar. Geol. 189 (2002) 343–370.
[42] G.R. Lucchi, M. Rebesco, Glacial contourites on the Antarctic Peninsula margin: insight for palaeoenvironmental and palaeoclimatic conditions, In: Economic and Palaeoceanographic

Importance of Contourites, A. Viana, M. Rebesco (Eds.), Geological Society of London Special Publication 276 (in press).
[43] C.J. Pudsey, A. Camerlenghi, Glacial–interglacial deposition on a sediment drift on the Pacific margin of the Antarctic Peninsula, Antarct. Sci. 10 (1998) 286–308.
[44] C.J. Pudsey, Sedimentation on the continental rise west of the Antarctic Peninsula over the last three glacial cycles, Mar. Geol. 167 (2000) 313–338.
[45] G. Villa, D. Persico, M.C. Bonci, R.G. Lucchi, C. Morigi, M. Rebesco, Biostratigraphic characterization and Quaternary microfossil palaeoecology in sediment drifts west of the Antarctic Peninsula—implications for cyclic glacial–interglacial deposition, Palaeogeogr. Palaeoclimatol. Palaeoecol. 198 (2003) 237–263 (26).
[46] EPICA community members, Eight glacial cycles from an Antarctic ice core, Nature 429 (2004) 623–628.
[47] B. Narcisi, J.R. Petit, B. Delmonte, I. Basile-Doelsch, V. Maggi, Characteristics and sources of tephra layers in the EPICA-Dome C ice record (East Antarctica): implications for past atmospheric circulation and ice core stratigraphic correlations, Earth Planet. Sci. Lett. 239 (2005) 253–265.
[48] J.L. Smellie, The upper Cenozoic tephra record in the south polar region: a review, Glob. Planet. Change 21 (1999) 51–70.
[49] H. Heinrich, Origin and consequences of cyclic ice rafting in the northeast Atlantic Ocean during the past 130,000 years, Quat. Res. 29 (1988) 142–152.
[50] G. Bond, H. Heinrich, W. Broecker, L. Labeyrie, J. McManus, J. Andrews, S. Huon, R. Jantschik, S. Clasen, C. Simet, K. Tedesco, M. Klas, G. Bonani, S. Ivy, Evidence for massive discharges of icebergs into the North Atlantic ocean during the last glacial period, Nature 360 (1992) 245–249.
[51] G. Bond, W. Broecker, S. Johnsen, J. McManus, L. Labeyrie, J. Jouzel, G. Bonani, Correlations between climate records from North atlanctic sediments and Greenland ice, Nature 365 (1993) 143–147.
[52] L. Sagnotti, P. Rochette, M. Jackson, F. Vadeboin, J. Dinarès-Turell, A. Winkler, "Mag-Net" Science Team, inter-laboratory calibration of low field and anhysteretic susceptibility measurements, Phys. Earth Planet. Inter. 138 (2003) 25–38.
[53] S.A. Brachfeld, C. Kissel, C. Laj, A. Mazaud, Viscous behavior of u-channels during acquisition and demagnetization of remanences: implications for paleomagnetic and rock-magnetic investigations, Phys. Earth Planet. Inter. 145 (2004) 1–8.
[54] J.L. Kirschvink, The least-square line and plane and the analysis of paleomagnetic data, Geophys. J. R. Astron. Soc. 62 (1980) 699–718.
[55] C.G. Langereis, M.J. Dekkers, G.J. De Lange, M.E. Patern, P.J.M. Van Santvoort, Magnetostratigraphy and astronomical calibration of the last 1.1 Myr from an eastern Mediterranean piston core and dating of short events in the Brunhes, Geophys. J. Int. 129 (1997) 75–94.
[56] S.P. Lund, G. Acton, B. Clement, M. Hastedt, M. Okada, R. Williams, Geomagnetic field excursions occurred often during the last million years, Eos, Trans. Am. Geophys. Union 79 (1998) 178–179.
[57] B.S. Singer, M.K. Relle, K.A. Hoffman, A. Battle, C. Laj, H. Guillou, J.C. Carracedo, Ar/Ar ages from transitionally magnetized lavas on La Palma, Canary Islands, and the geomagnetic instability timescale, J. Geophys. Res. 107 (B11) (2002) 2307, doi:10.1029/2001JB001613.
[58] H. Oda, H. Shibuya, Deconvolution of long-core paleomagnetic data of Ocean Drilling Program by Akaike's Bayesian Information Criterion minimization, J. Geophys. Res. 101 (1996) 2815–2834.
[59] Y. Guyodo, J.E.T. Channell, R. Thomas, Deconvolution of u-channel paleomagnetic data near geomagnetic reversals and short events, Geophys. Res. Lett. 29 (17) (2002) 1845, doi:10.1029/2002GL014927.
[60] J.W. King, S.K. Banerjee, J. Marvin, A new rock-magnetic approach to selecting sediments for geomagnetic paleointensity for the last 4000 years, J. Geophys. Res. 88 (B7) (1983) 5911–5921.
[61] L. Tauxe, Sedimentary records of relative paleointenstiy of the geomagnetic field: theory and practice, Rev. Geophys 31 (1993) 319–354.
[62] J.-P. Valet, L. Meynadier, Geomagnetic field intensity and reversals during the past four million years, Nature 366 (1993) 234–238.
[63] J.-P. Valet, L. Meynadier, A comparison of different techniques for relative paleointensity, Geophys. Res. Lett. 25 (1998) 89–92.
[64] J.-P. Valet, Time variations in geomagnetic intensity, Rev. Geophys. 41 (2003) 1/1004, doi:10.1029/2001RG000104.
[65] D. Paillard, L. Labeyrie, P. Yiou, Macintosh program performs time-series analysis, Eos, Trans. Am. Geophys. Union 77 (1996) 397.
[66] R. Thompson, F. Oldfield, Environmental Magnetism, Allen and Unwin, London, 1986.
[67] N. Thouveny, J.-L. Beaulleu, E. Bonifay, K.M. Creer, J. Guiot, M. Icole, S. Johnsen, J. Jouzel, M. Reille, T. Williams, D. Williamson, Climate variations in Europe of the past 140 kyr deduced from rock magnetism, Nature 371 (1994) 503–506.
[68] K.L. Verosub, A.P. Roberts, Environmental magnetism: past, present and future, J. Geophys. Res. 100 (1995) 2175–2192.
[69] M.J. Dekkers, Environmental magnetism: an introduction, Geol. Mijnb. 76 (1997) 163–182.
[70] J.S. Stoner, J.T. Andrews, The North Atlantic as a Quaternary magnetic archive, in: B.A. Maher, R. Thompson (Eds.), Quaternary Climates, Environments and Magnetism, UK Cambridge University press, 1999, pp. 49–80.
[71] B.A. Maher, R. Thompson, M.W. Hounslow, Introduction, in: B.A. Maher, R. Thompson (Eds.), Quaternary Climates, Environments and Magnetism, UK Cambridge University press, 1999, pp. 1–48.
[72] J.W. King, S.K. Banerjee, J. Marvin, Ö. Özdemir, A comparison of different magnetic methods for determining the relative grain size of magnetite in natural materials: some results from lake sediments, Earth Planet. Sci. Lett. 59 (1982) 404–419.
[73] J. Bloemendal, J.W. King, F.R. Hall, S.-J. Doh, Rock magnetism of Late Neogene and Pleistocene deep-sea sediments: relationship to sediment source, diagenetic processes, and sediment lithology, J. Geophys. Res. 97 (1992) 4361–4375.
[74] B.A. Maher, R. Thompson, Paleoclimatic significance of the mineral magnetic record of the Chinese loess and paleosols, Quat. Res. 37 (1992) 155–170.
[75] S.K. Banerjee, J. King, J. Marvin, A rapid method for magnetic granulometry with applications to environmental studies, Geophys. Res. Lett. 8 (1981) 333–336.
[76] R.A. Berner, Sedimentary pyrite formation, Am. J. Sci. 268 (1970) 1–23.
[77] R.A. Berner, Sedimentary pyrite formation: an update, Geochim. Cosmochim. Acta 48 (1984) 605–615.
[78] S.J. Kao, C.S. Horng, K.K. Liu, A.P. Roberts, Carbon–sulfur–iron relationships in sedimentary rocks from Southwestern

Taiwan: influence of geochemical environment on greigite and pyrrhotite formation, Chem. Geol. 203 (2004) 153–168.

[79] R. Day, M. Fuller, V.A. Schmidt, Hysteresis properties of titanomagnetites. Grain-size and compositional dependence, Phys. Earth Planet. Inter. 13 (1977) 260–267.

[80] D.J. Dunlop, Theory and application of the day plot (M_{RS}/M_S versus H_{CR}/H_C). 1. Theoretical curves and tests using titanomagnetite data, J. Geophys. Res. 107 (2002), doi:10.1029/2001JB000486.